

Environmental durability of phosphoric acid anodized aluminium adhesive joints protected with hydration inhibitors

D. A. HARDWICK*, J. S. AHEARN†, A. DESAI, J. D. VENABLES
*Martin Marietta Corporation, Martin Marietta Laboratories, 1450 South Rolling Road,
 Baltimore, Maryland 21227, USA*

An adsorbed monolayer of the organic inhibitor nitrilotris methylene phosphonic acid (NTMP) improves the bond durability of 2024 aluminium adherends prepared by phosphoric acid anodization (PAA). As had previously been determined for Forest Products Laboratories (FPL)-prepared adherends, maximum improvements occurred when a monolayer of NTMP was adsorbed onto the surface. Examination of the wedge test failure surfaces of PAA adherends treated in NTMP revealed that although crack propagation had initially involved oxide to hydroxide conversion of the original PAA oxide, the locus of failure transfers to the adhesive near the surface quite early in the test. This means that the failure of NTMP-treated PAA adherends was predominantly cohesive through the adhesive.

1. Introduction

Adhesively-bonded aluminium structures are finding increasing use in numerous applications that call for a lightweight structural material. The performance of such structures is largely determined by two factors: the initial bond strength of the adherend/adhesive interface and the stability of the interface in a humid environment, i.e. the durability of the bond. Recent studies [1] have indicated that the initial bond strength of joints produced by commercial aerospace bonding processes, including the Forest Products Laboratory (FPL) process and the Boeing phosphoric acid anodization (PAA) process, is determined principally by physical interlocking of the oxide on the aluminium adherend with the adhesive. On the other hand, the long-term durability of the aluminium oxide adhesive bond appears to depend on the resistance of the original adherend oxide to conversion to a hydroxide in the presence of moisture [2].

The bond durability of adherends prepared using the PAA process is substantially better than that of adherends prepared with the FPL process. PAA oxides not only are considerably thicker than FPL oxides (≈ 300 nm compared to 40 nm [1]) but they also contain phosphorus in the form of a phosphate, a known inhibitor of aluminium oxide hydration [3]. Moreover, recent work [4] has shown that a critical step in the hydration of PAA oxides is the dissolution of a phosphorus-rich surface layer.

It has been shown that the adsorption of phosphorus-containing compounds onto FPL aluminium oxides stabilizes the oxide by increasing the time needed to convert the original oxide into a hydroxide [5]. This increase in the stability of the FPL

oxide appears to be translated directly into improvements in bond durability. For example, adsorption of approximately a monolayer of the organic inhibitor species, nitrilotris methylene phosphonic acid (NTMP), $N[CH_2P(O)(OH)_2]_3$ onto FPL-prepared 2024 aluminium adherends improved their bond durability to the point where they rivalled the durability of adherends prepared with the PAA process [6]. Analysis of the results on FPL-prepared adherends after treatment in a variety of inhibitors suggested that an inhibitor's effectiveness depended on its ability to both inhibit the conversion of aluminium oxide to the hydroxide and to form chemical bonds with the adhesive [6].

We have extended the use of the inhibitor NTMP to PAA-prepared adherends, whose bond durability is superior to FPL-prepared adherends, a consequence of a thicker oxide film and the increased resistance of the oxide to hydration. Nevertheless, in the presence of moisture, the PAA oxide hydrates, and bond strength is degraded. The adsorption of a monolayer of inhibitor molecules onto the oxide surface might improve hydration resistance without compromising initial bond strength and, at the same time, might improve the strength of chemical bonds between the oxide and the adhesive.

2. Experimental techniques

2.1. Sample preparation

All test coupons and panels were first degreased in a commercial alkaline cleaning solution and then rinsed in distilled, deionized water. Degreasing was followed by a standard FPL treatment, consisting of a 15 min immersion in an agitated aqueous solution of sodium

*Present address: Los Alamos National Laboratory, Los Alamos, New Mexico 86545, USA.

†Author to whom correspondence should be sent.

dichromate dihydrate (60 g l^{-1}) and sulphuric acid (17% v/v) held at 65°C ; another rinse in distilled, deionized water; and air drying. The FPL-treated samples then underwent the PAA process; anodization in a 10% phosphoric acid solution at a potential of 10 V and a temperature of 20 to 25°C for 20 min; followed by a rinse in distilled, deionized water; and air drying.

Inhibitor treatment of panels was accomplished by 30 min immersion in an aqueous solution of the inhibitor held at either room temperature or 80°C ; a rinse in distilled, deionized water; and air drying. The inhibitor used was nitrilotris methylene phosphonic acid (NTMP): $\text{N}[\text{CH}_2\text{P}(\text{O})(\text{OH})_2]_3$.

2.2. Wedge-test procedure.

Following surface preparation, adherends ($15\text{ cm} \times 15\text{ cm} \times 0.3\text{ cm}$) were bonded together using American Cyanamide FM 123-2 adhesive cured at 120°C for 1 h. The adhesive consists of a Dacron mat impregnated with an epoxy based resin. These bonded panels were cut into five $2.5\text{ cm} \times 15\text{ cm}$ test pieces and wedges (0.32 cm thick) were inserted between the two adherends to provide a stress at the bondline. After an equilibration period of 1 h at ambient conditions, the test samples were placed in a humidity chamber held at 60°C and 98% r.h. Periodically, the test pieces were removed from the chamber and examined under an optical microscope to locate and mark the position of the crack front. When the test was complete, usually after 150 to 160 h, callipers were used to measure the positions of the marks, which denoted length as a function of time.

Wedge-test specimens are the adhesive-joint analogue of the wedge-force loaded double cantilever beam (DCB) specimen used in the testing of homogeneous materials. Using a combination of a simple beam theory and linear elastic fracture mechanics [7], the "energy release rate" or "crack extension force" G is given by

$$G = \frac{3h^3 Ew^2}{16a^4} \quad (1)$$

where E = Young's modulus of the adherends, h = thickness of the adherends, w = wedge thickness, and a = crack length, measured from the point of load application. This equation can be modified to take into account such factors as ductile strain in the adhesive which would allow rotation of the adherends ahead of the crack tip [8]. Because the test was used in a comparative way only and the same adhesive was always employed, such corrections were not used in this analysis of the wedge-test data.

Using the crack length data generated by the wedge test, G was calculated using Equation 1. The average crack velocity, V , was also determined from the information on crack length as a function of time.

2.3. Surface analysis

Surface analysis measurements were done with a Physical Electronics (Model 548) spectrometer equipped with a double pass cylindrical mirror analyser. Measurements were taken in either the

X-ray photoelectron spectroscopy (XPS) or Auger electron spectroscopy (AES) modes, the latter being used in conjunction with sputter-etching (argon ions) to obtain information on compositions as a function of depth.

Test coupons were analysed using XPS to determine the amount of inhibitor adsorbed on the oxide surface. The peak heights of the 2p photoelectrons of phosphorus and aluminium were measured and the phosphorus/aluminium (P/Al) ratio calculated using previously determined sensitivity factors [4]. The P/Al ratio was taken as a measure of the relative coverage of inhibitor on the aluminium-oxide surface. On completion of wedge-tests, the matching failure surfaces were separated and samples selected for surface analysis. Again, the reported analyses were determined from peak height measurements using sensitivity factors derived from standards. Auger depth-profiling was performed on selected failure surfaces.

2.4. Scanning electron microscopy (SEM)

Surfaces were examined in a JEOL-100CX scanning transmission electron microscope (STEM) operated in the high resolution (3 nm) SEM mode. To suppress charging of the surface by the electron beam, an extremely thin platinum coating was deposited on the surface of the specimens by secondary ion deposition.

3. Results

3.1. Inhibitor surface coverage

The inhibitor surface coverage (P/Al ratio) on PAA oxide surfaces as a function of inhibitor solution concentration indicates that saturation surface coverage is achieved with solution concentrations above 10 p.p.m. NTMP (Fig. 1). Surface coverage obtained with NTMP solutions at 80°C yield P/Al ratios more than double those obtained at room temperature. For example, a 300 p.p.m. solution at 80°C produces a P/Al ratio = 0.49 ± 0.04 .

3.2. Wedge tests

The wedge-test results (Fig. 2) for FPL adherends, PAA-adherends, and PAA-adherends treated with low (10 p.p.m.) and high (300 p.p.m.) concentration NTMP solutions demonstrate that the bond durability of PAA-adherends is better than that of FPL-adherends and that the durability can be further improved by pretreatment with NTMP. As the figure shows surface treatment in a 300 p.p.m. NTMP solution gave little further improvement, as gauged by final crack length, over treatment in a 10 p.p.m. solution. This probably results from the similar surface coverage obtained by treatment in 10 and 300 p.p.m. solutions.

In Fig. 3, wedge-tests results have been plotted for adherends treated in 300 p.p.m. NTMP solution at two temperatures, ambient and 80°C . In the high concentration (300 p.p.m.) solution at 80°C , there was a decrease in bond durability compared with similar treatment at room temperature.

In a separate set of wedge-tests (Fig. 4), adherends treated in 10 p.p.m. NTMP did not behave as well as those shown in Fig. 2. Saturation surface coverage is

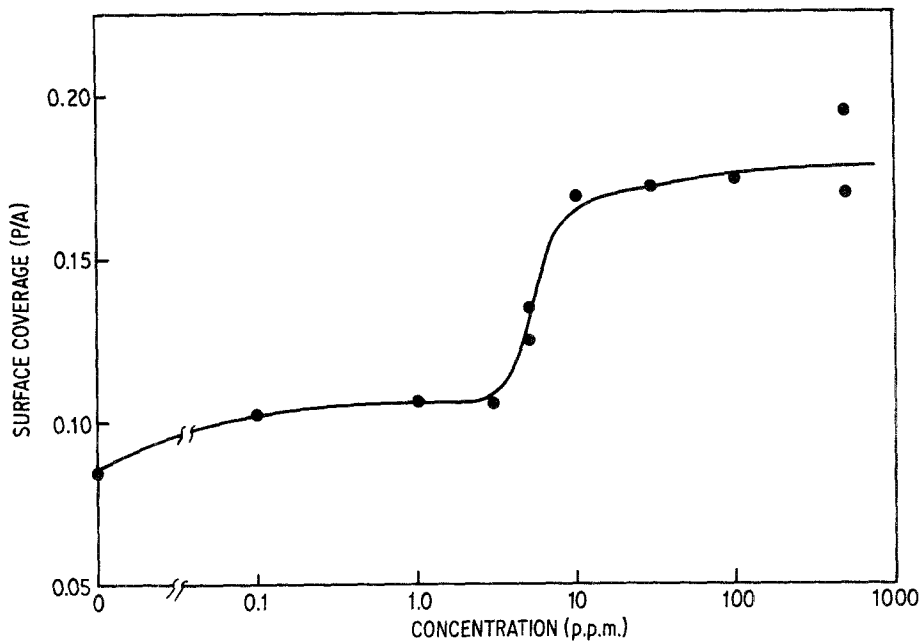


Figure 1 Surface coverage of NTMP-treated PAA oxide surface as a function of NTMP solution concentration at room temperature.

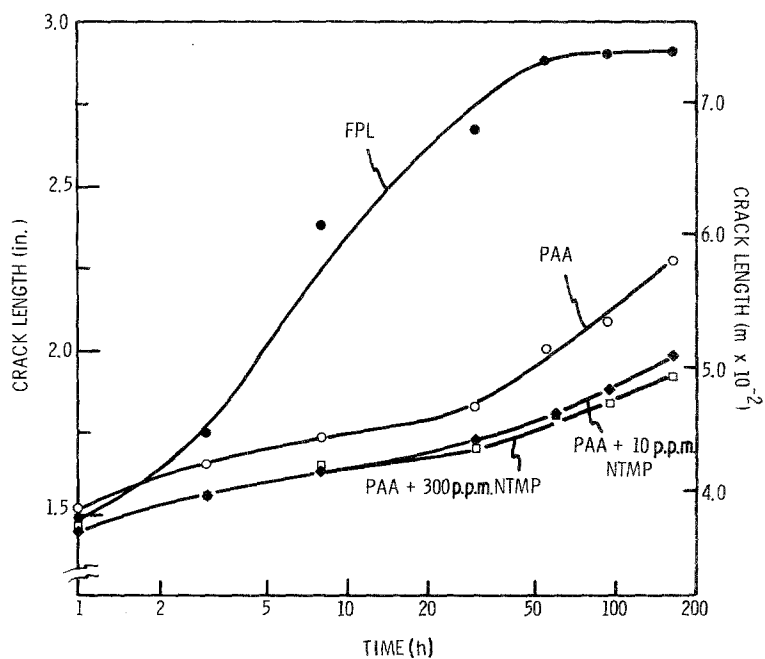


Figure 2 Crack length against time for FPL-adherends and PAA-adherends and PAA-adherends treated as shown on the graph.

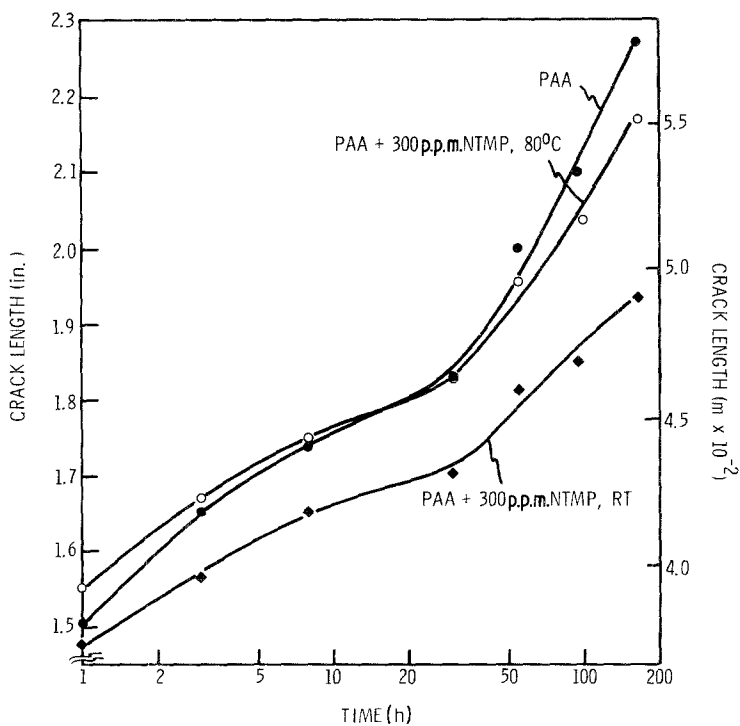


Figure 3 Crack length against time for PAA-adherends treated as marked on the graph.

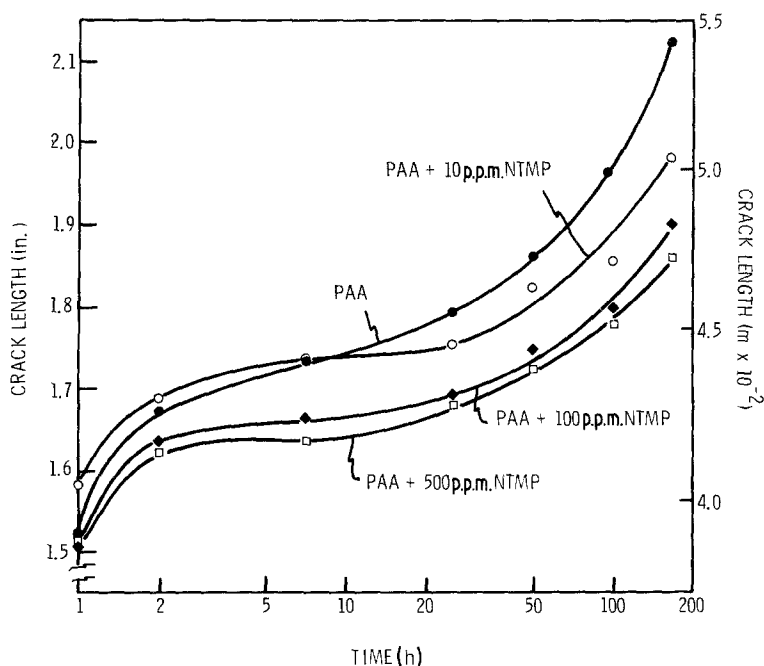


Figure 4 Crack length against time for PAA-adherends treated as marked on the graph.

not always achieved after treatment in 10 p.p.m. solutions, probably because small fluctuations in adsorption efficiency result in significant variations in surface coverage in this solution range. Hence, wedge-test performance will vary because of the variations in inhibitor coverage. However, once saturation coverage is established (100 p.p.m. solution treatments), the results are highly reproducible. In addition to the results for adherends treated in 100 and 500 p.p.m. NTMP solutions (reported in Fig. 4.), tests were also conducted using PAA-adherends treated in 200 and 300 p.p.m. NTMP solutions. The same behaviour within experimental scatter was seen in all of these panels, indicating that optimal performance is achieved with monolayer NTMP coverage.

As outlined in the experimental procedure (see Section 2.2.), the wedge-tests results were analysed to

yield crack extension forces and resultant crack velocities. In the plots seen in Figs. 5 and 6, G decreases over the duration of the test. Thus, initial G values are on the right hand side of the graph. In Fig. 5 these results are plotted for FPL-treated and PAA-treated adherends and in Fig. 6 for PAA adherends treated in 100 to 500 p.p.m. NTMP solutions. Data for the adhesive, FM 123-2, which was obtained using PAA-adherends sprayed with a corrosion inhibiting primer prior to bonding, are also included. Because the crack was completely cohesive through the centre of the adhesive layer in this case, the wedge-test provided information on the fracture behaviour of the adhesive alone.

3.3. SEM examination of fracture surfaces

At the conclusion of the humidity exposure, the

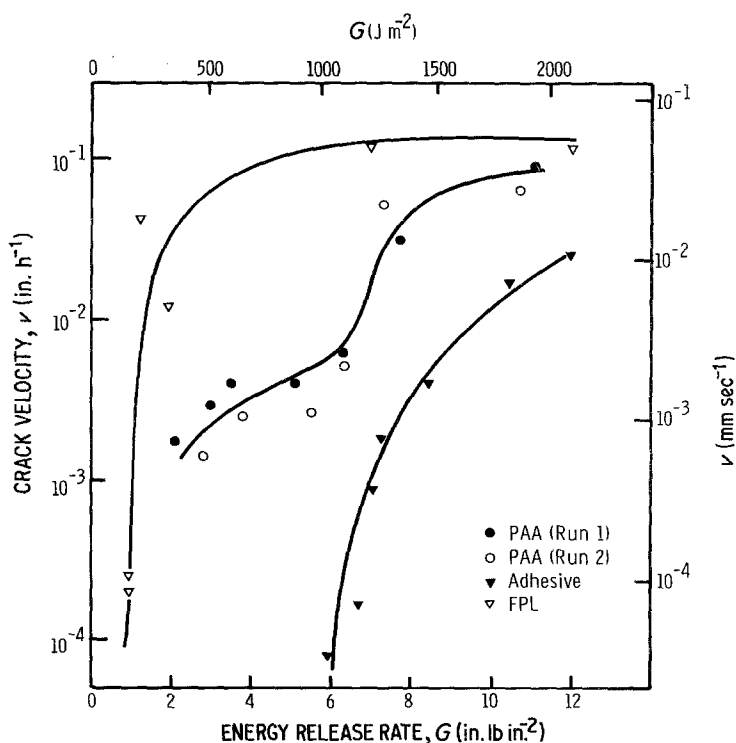


Figure 5 Crack velocity against energy release rate for FPL, PAA and FM123-2 adhesive.

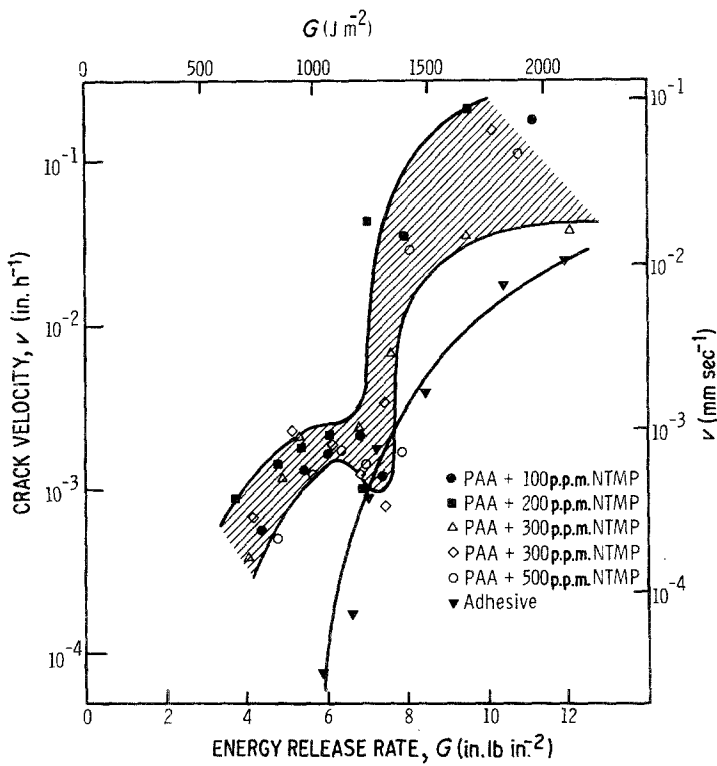


Figure 6 Crack velocity against energy release rate for NTMP-treated PAA-adherends and FM123-2 adhesive.

wedge-test assemblies were separated. SEM examination confirmed, as previously reported for FPL-adherends [6], that once a warm humid environment was established at the crack tip, a new crack was initiated at the oxide/adhesive interface. This always occurred, even on PAA-adherends treated in high concentrations of inhibitor solution. The re-initiation and initial propagation of the crack was associated with conversion of the original oxide to boehmite.

Visual examination of the adherends indicated that the crack path was not confined exclusively to one oxide/adhesive interface. Furthermore, the failure sur-

face where the initial crack propagated looked dull or stained, but near the final crack tip the failure surface on the aluminium side was shiny and had a slight purple sheen. SEM examination of the aluminium side of the fracture surface revealed that the dull regions corresponded to a hydrated surface, and the shiny regions corresponded to an oxide surface coated with a thin adhesive layer; the transition from dull to shiny occurred during the final increment of crack movement. Fig. 7a is a schematic view of the overall surface. The surface away from the crack tip had the "cornflake" morphology of boehmite as shown in Fig. 7b,

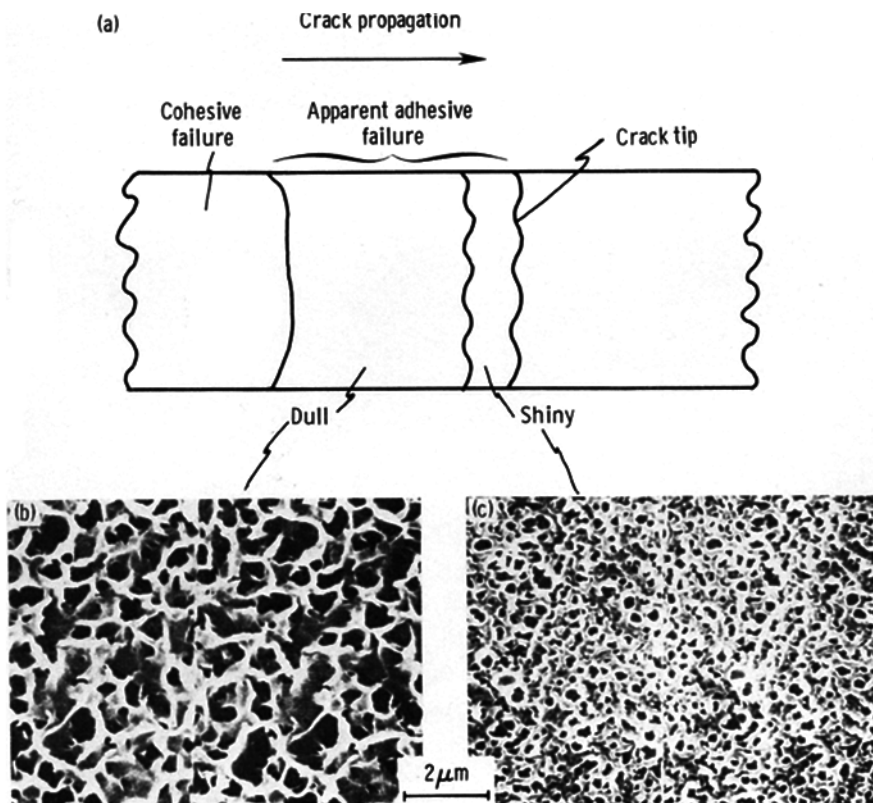
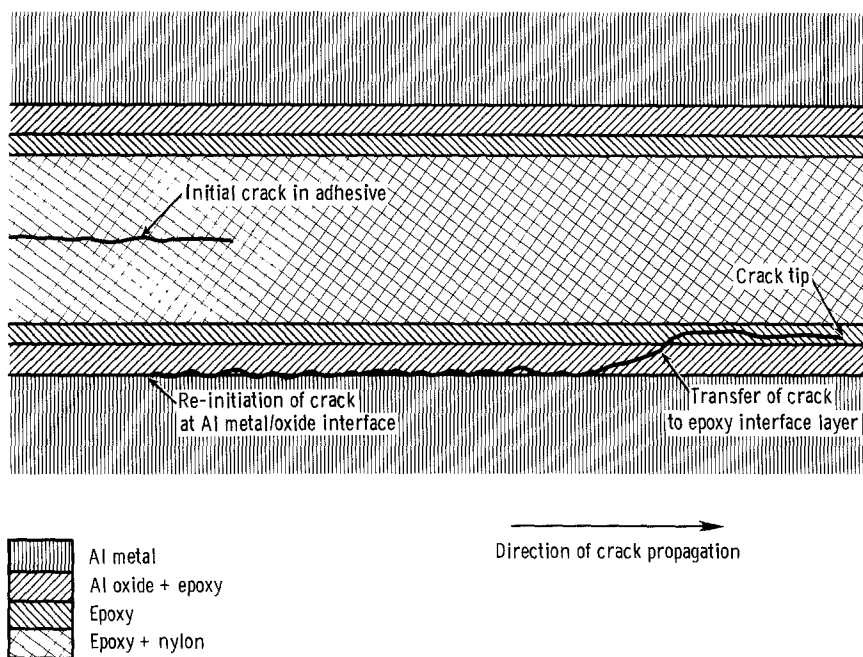


Figure 7 Fracture surface of wedge-test sample from untreated PAA-adherends (a) schematic of surface, (b) STEM stereo micrograph from dull area and (c) STEM stereo micrograph from shiny area.

Figure 8 Schematic of crack path in wedge-test samples.



whereas the surface at the crack tip exhibited the morphology of failed adhesive (Fig 7c). Since there was no evidence of the Dacron mat on the failure surfaces, the crack evidently progressed in the epoxy resin between the oxide surface and the Dacron reinforced adhesive, as shown in Fig. 8.

At this point, conversion of oxide to hydroxide probably occurs at such a low rate that it no longer is a precursor to crack propagation, and propagation through the adhesive becomes a more favourable mechanism of crack growth. The crack moves progressively away from the interface region until it is wholly within the adhesive layers. The adhesive is deformed by the passage of the crack front until a deformation limit is exceeded, at which point it recoils to form the structure seen in Fig. 7c.

On PAA-treated adherends in the presence of the NTMP inhibitor, the transition region, indicating transfer of the crack path away from the oxide/adhesive interface, occurs much earlier. Figs. 9a and b show the fracture surface on the aluminium side of the adherend treated in a 200 p.p.m. solution of NTMP.

The crack has propagated through the adhesive but is still quite close to the interface as no fibres from the Dacron mat in the adhesive are observed. Because moisture was still available to the oxide, with the passage of sufficient time (judged from the position of this region on the fracture surface to be at least 100 h), the oxide under the adhesive has transformed to boehmite. In fact, sufficient time has elapsed to allow the formation of bayerite on top of the boehmite flakes and it can be seen distorting the adhesive layer in Fig. 9a. The cracks in the adhesive layer seen in Fig. 9 are also a direct result of oxide to hydroxide conversion. The formation of boehmite from the initial oxide involves a lattice expansion, and more importantly, the flake morphology adopted by boehmite is considerably more open than that of the original amorphous oxide. This results in a three-fold increase in the thickness of the layer under the adhesive [9], and the consequent strain produces cracks in the adhesive. The boehmite structure of the underlying layer is seen very clearly in Fig. 9b.

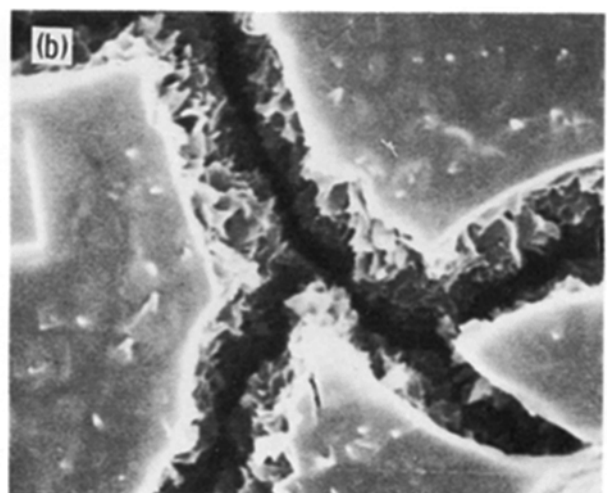
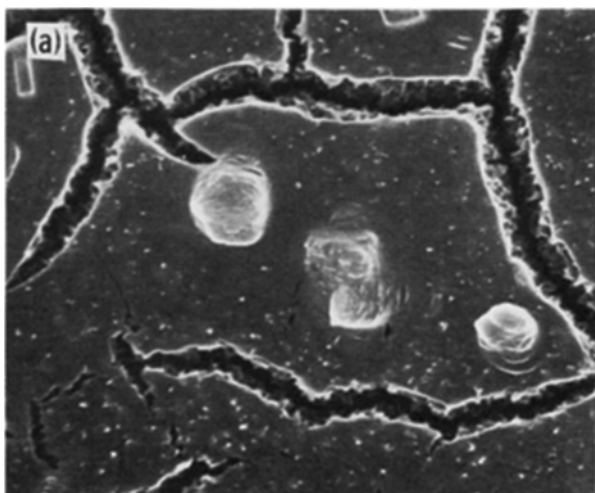


Figure 9 STEM micrographs of the aluminium side of wedge-test samples treated in 200 p.p.m. solution of NTMP, (b) is a higher magnification of (a).

TABLE I Surface composition of the aluminium side of wedge-test failures as determined by XPS

Surface preparation (appearance)	Composition (%)		
	Al	O	C
FPL	16	52	32
PAA (Dull)	22	46	32
PAA (Shiny)	3	18	79

3.4. Surface analysis

Dull and shiny aluminium-side fracture surfaces on PAA-adherends were analysed by XPS and compared with results from an FPL-adherend fracture surface (Table I). The dull PAA fracture surface was very close in composition to the FPL failure surface. This result is not surprising because both surfaces are identical in appearance, being covered with the corn-flake structure of boehmite. The shiny surface, on the other hand, exhibited a very low aluminium concentration and a high oxygen concentration, confirming the SEM evidence that the shiny regions appear to be ruptured adhesive.

AES depth profiling further confirmed these results. The aluminium-hydroxide layer on the dull sample was ~ 500 nm thick (Fig. 10). Undulations in the aluminium and oxygen concentrations with depth may be due to density changes in the hydroxide layer but may also result from the sputtering process on the extremely thick hydroxide layer.

The oxide layer on the shiny surface was ~ 100 nm thick (Fig. 11), as evidenced by the decrease in oxygen concentration after 30 min sputtering. Considerable carbon was also observed on the surface, undoubtedly a result of the adhesive that penetrated into the pores of the oxide when the bond was first formed. Previous work [10], using AES depth profiling has shown that the thickness of a typical PAA-oxide is ~ 100 nm. Thus, it appears that the shiny aluminium fracture surface consisted of a very thin adhesive layer overlying the original PAA-oxide.

4. Discussion

The range of NTMP solution concentrations used to treat PAA surfaces was identical to that used in our previously reported studies to treat FPL surfaces [6]. Despite the fact that the P/Al ratio of the PAA oxide

is 0.1 compared with zero for an FPL oxide, both oxides have P/Al ratio of 0.15 to 0.20 following saturation treatment in NTMP solutions at room temperature. This phenomenon is duplicated in the 80°C treatment since at a solution concentration of 300 p.p.m., the surface coverage for both FPL and PAA oxides is in the range of 0.4 to 0.5. The high surface coverage obtained on FPL surfaces treated in NTMP solutions at 80°C is most likely related to multilayer surface coverages [6]; this is probably also true for PAA surfaces treated in a similar fashion.

In addition, the surface coverage for FPL oxide treated in phosphoric acid solution at room temperature saturates at $\text{P/Al} = 0.1$, [6] i.e. at the same coverage level that occurs on PAA surfaces. This result implies that the surface active sites on the PAA oxide are initially occupied by phosphorus-containing groups derived from phosphoric acid. Treatment in room temperature NTMP solutions results in NTMP groups adsorbing onto the pre-existing surface or replacing at least some of the initial phosphorus-containing groups. Although both processes increase the surface coverage, as measured by the P/Al ratio, our present experimental results do not allow us to distinguish between them.

The wedge-test results demonstrate that the bond durability of PAA-treated adherends can be increased by pretreatment in NTMP inhibitor solutions. This behaviour might result if bonds to the Al_2O_3 surfaces, formed by the NTMP molecule, are more moisture resistant than those formed by the PA molecule, i.e. the stability of the PAA surface against hydration would be increased. The increase in the P/Al ratio after NTMP treatment suggests that NTMP either displaces PA molecules already adsorbed on the surface or attaches to unoccupied surface sites. In either case, the increased P/Al ratio should improve the stability of the PAA oxide in a moist environment and improve bond durability.

Alternatively, if the NTMP molecule forms stronger chemical bonds to the epoxy adhesive than PA, the NTMP-adhesive interface would be strengthened and PAA bond durability would be improved. Previous work has shown that the NTMP molecule improves both FPL oxide stability and bond durability whereas the PA molecule only improves oxide stability [6]. This

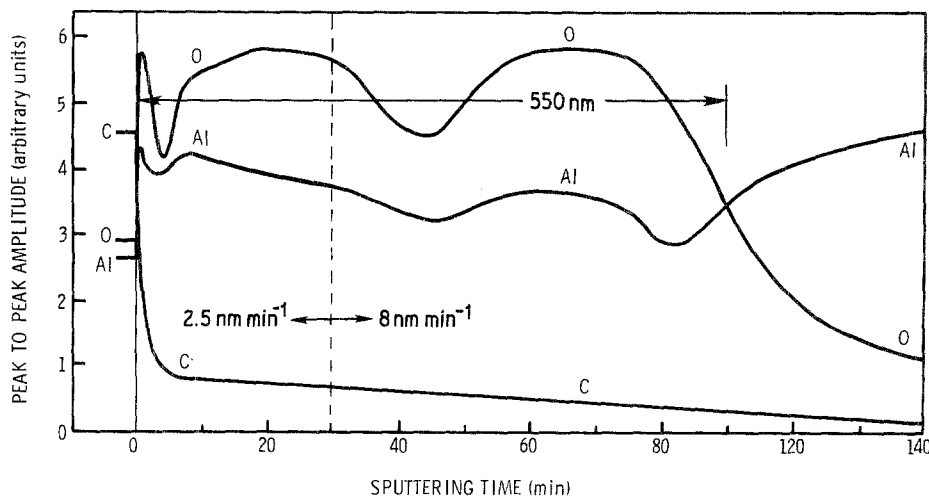


Figure 10 Depth profile of "dull" region on the aluminium side of PAA wedge-test failure surface.

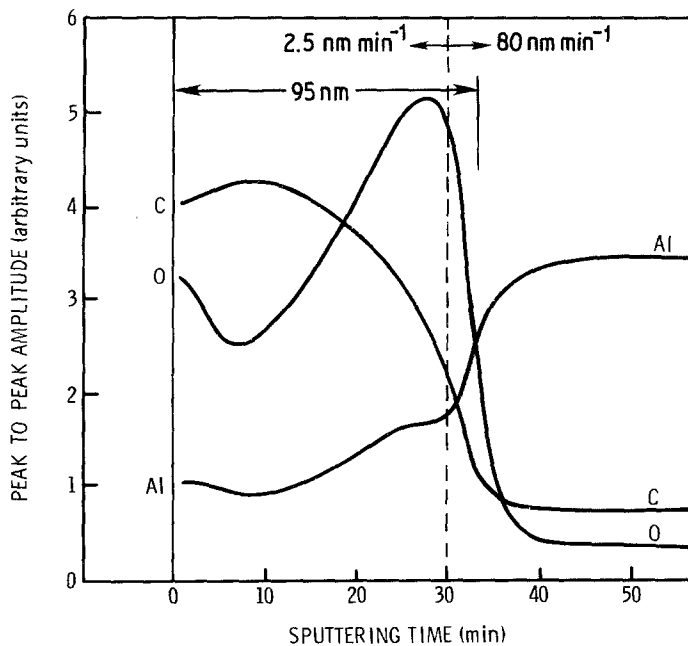


Figure 11 Depth profile of "shiny" region on the aluminium side of PAA wedge-test failure surfaces.

implies that the NTMP molecule not only stabilizes the oxide, but perhaps also acts more effectively to chemically couple the oxide and adhesive.

Maximum increases in PAA bond durability occurred when a monolayer of the NTMP inhibitor was present on the surface. Treatment of PAA in an 80°C 300 p.p.m. NTMP solution increased surface coverage 1.45 times over the level recorded for a similar treatment at room temperature, but the multilayer coverage did not further improve bond durability. Similar results were obtained previously with FPL adherends [6]. In that work, analysis of the FPL failure surfaces revealed that P was present on both sides of the failure, implying that the crack passed through the multilayer surface film produced by the elevated temperature treatment. Similar mechanisms may be operative when PAA-adherends have multiple NTMP layers between the oxide and the adhesive. Failure can occur at least partially through the NTMP layers so that bond durability is worse than with a monolayer NTMP coverage, although still better than untreated PAA-adherends.

When the wedge-test data is analysed using the fracture mechanics approach outlined in Section 2.2. it is clear that adherend behaviour is strongly dependent on surface treatment prior to bonding. This is illustrated in Figs. 5 and 6, which include data for adherend surfaces treated with FPL, PAA, PAA + NTMP, and the adhesive. Insertion of the wedge-test assemblies into the warm humid environment resulted in the initiation of a crack at or near the adhesive/oxide interface. As previously reported [6], there is an abrupt transition on FPL-adherends particularly, from cohesive to adhesive failure during the first hour of exposure to the humid environment. This transition is less abrupt for the PAA-adherends and, on PAA-treated with saturation surface coverages of NTMP, there is effectively an "incubation period" before interfacial failure is observed.

The initiation and propagation of the interface crack is apparently due to direct hydration of the oxide or weakening of the adhesive-inhibitor inter-

face and the associated breakdown of interface integrity. If cohesive failure is forced by using a corrosion inhibiting primer prior to bonding, then optimum bond durability for our test system can be achieved because only the adhesive behaviour under stress in a warm, humid environment is involved.

Once interfacial cracking has begun on FPL-adherends, the initial crack velocity (V) is maintained to very low G values, indicating that the mechanism of crack growth is independent of the stress (Fig. 5). Indeed, the conversion of oxide to hydroxide is such a stress-independent mechanism, which SEM examination of fracture surfaces had previously identified as the mechanism by which adhesive bonds fail in the presence of moisture [2].

The behaviour of PAA-adherends is quite different. At G levels that are still relatively high, the crack velocity falls two orders of magnitude below its initial value. SEM examination of these fracture surfaces (see Section 3.3.) revealed that in the course of the wedge-test the locus of failure is initially through the oxide close to the adhesive interface, in latter stages, it goes through the adhesive near this interface.

On PAA-adherends treated in higher concentrations of NTMP solutions, this transfer into the adhesive layer near the interface occurs quite early in the test. The discontinuity in the behaviour of these adherends evident in Figs. 5 and 6 is probably a reflection of this change in the locus of failure. The behaviour at the higher G levels is evidence of failure of the adherend through oxide hydration, whereas at the lower G levels it is characteristic of the adhesive near the interface. The $V-G$ curve for the inhibited PAA-adherends approaches that of the adhesive. The crack velocity does not follow the adhesive curve because the locus of failure is in the near interface region where the adhesive is not Dacron mat reinforced.

Our evidence shows that the unreinforced adhesive is not as durable as the reinforced adhesive. The failure of the crack to transfer to the near interfacial region in the cohesive tests suggests that an activation

energy for crack transfer or crack re-initialization is necessary. Otherwise the crack would not have remained in the Dacron-reinforced adhesive.

Acknowledgements

We gratefully acknowledge Dr G. D. Davis for several useful comments and his critical review of the text. The financial support of the Office of Naval Research, Washington, DC, and the Army Research Office, Durham, NC, under contract number N00014-80-C-0718, is appreciated.

References

1. J. D. VENABLES, D. K. McNAMARA, J. M. CHEN, T. S. SUN and R. L. HOPPING, *Appl. Surf. Sci.* **3** (1979) 88.
2. J. D. VENABLES, D. K. McNAMARA, J. M. CHEN, B. M. DITCHEK, T. I. MORGENTHALER and T. S. SUN, Proceedings of the 12th National SAMPE Technical Conference (SAMPE, Azusa, California, 1980) p. 909.
3. D. A. VERMILYEA and W. VEDDER, *Trans. Faraday Soc.* **66** (1970) 2644.
4. G. D. DAVIS, T. S. SUN, J. S. AHEARN and J. D. VENABLES, *J. Mater. Sci.* **17** (1982) 1809.
5. J. S. AHEARN, G. D. DAVIS, T. S. SUN and J. D. VENABLES, in "Adhesion Aspects of Polymer Coatings", edited by K. Mittal (Plenum Press, New York) p. 281.
6. D. A. HARDWICK, J. S. AHEARN, and J. D. VENABLES, *J. Mater. Sci.* **19** (1984) 223.
7. D. BROEK, "Elementary Engineering Fracture Mechanics" (Sijthoff and Noordhoff, Alphen aan den Rijn, Netherlands, 1978) p. 154.
8. M. H. STONE and T. PEET, Royal Aircraft Establishment, Technical Memo MAT 349, July, 1980.
9. T. S. SUN, D. K. McNAMARA, J. S. AHEARN, J. M. CHEN, B. DITCHEK and J. D. VENABLES, *Appl. Surf. Sci.* **5** (1980) 406.
10. J. S. AHEARN, T. S. SUN, C. FROEDE and J. D. VENABLES, in Proceedings of ASM/SAMPE Conference on Specialized Cleaning Finishing and Coating Processes (Los Angeles, CA, 1980) also *SAMPE Quarterly* **12** (1980) 39.

*Received 16 January
and accepted 11 February 1985*